



# Sporadic vs. basal cell nevus syndrome associated odontogenic keratocysts: focus on CT and MRI including DWI

Hirota Muraoka<sup>1</sup> · Takashi Kaneda<sup>1</sup> · Takumi Kondo<sup>1</sup> · Yuta Kohinata<sup>1</sup> · Satoshi Tokunaga<sup>1</sup>

Received: 4 November 2024 / Accepted: 10 December 2024 / Published online: 20 December 2024  
© The Author(s) under exclusive licence to Japanese Society for Oral and Maxillofacial Radiology 2024

## Abstract

**Purpose** This study aimed to evaluate odontogenic keratocysts associated with basal cell nevus syndrome (BCNS) using computed tomography (CT) and magnetic resonance imaging (MRI) including diffusion-weighted imaging (DWI) and compare them with sporadic cases.

**Materials and methods** This study investigated 17 outpatients who underwent panoramic radiography, CT, and MRI between August 2012 and January 2021. Five of these patients had BCNS had 16 odontogenic keratocysts, for which the authors recorded detailed findings. DWI analysis compared the apparent diffusion coefficient (ADC) values of odontogenic keratocysts in patients with BCNS and sporadic cases. The Mann–Whitney test was used to analyse bivariate statistics.

**Results** Patients with BCNS had an average of 3.2 lesions in the jaw. On DWI, the ADC value ranged from 0.58 to  $2.66 \times 10^{-3}$  mm<sup>2</sup>/s. The values for sporadic odontogenic keratocysts ranged from 0.67 to  $1.11 \times 10^{-3}$  mm<sup>2</sup>/s. The median values were 0.94 and 0.89 for BCNS-associated and sporadic odontogenic keratocysts cases, respectively ( $P = .478$ ).

**Conclusion** This study presented detailed imaging findings of odontogenic keratocysts in patients with BCNS. Furthermore, the authors revealed a wide range of ADC values for BCNS-associated odontogenic keratocysts.

**Keywords** Basal cell nevus syndrome · Sporadic odontogenic keratocysts · CT · MRI · DWI

## Abbreviations

BCNS	Basal cell nevus syndrome
BCCs	Basal cell carcinomas
OKCs	Odontogenic keratocysts
CT	Computed tomography
MRI	Magnetic resonance imaging
DWI	Diffusion-weighted imaging
FOV	Field of view
HU	Hounsfield unit
STIR	Short-tau inversion recovery
TR	Repetition time
TE	Echo time
TI	Inversion time
ADC	Apparent diffusion coefficient

## Introduction

Basal cell nevus syndrome (BCNS), also known as Gorlin syndrome, is a rare autosomal dominant disorder characterized by the development of multiple basal cell carcinomas (BCCs) and other features, such as palmar and plantar pits, odontogenic keratocysts (OKCs), and skeletal abnormalities [1, 2]. This syndrome is caused by mutations in the protein patched homolog gene [3]. BCNS is passed down in an autosomal dominant pattern with high penetrance and variable expression, and its estimated prevalence is 1 per 60,000 persons [4–7]. OKCs are early manifestations of BCNS; however, some patients with BCNS with multiple OKCs may remain undiagnosed [8, 9]. Furthermore, patients with BCNS are at high risk of developing malignant lesions such as BCCs and medulloblastoma, necessitating early diagnosis and regular medical surveillance.

Distinguishing BCNS-associated OKCs from sporadic OKCs can be aided by clinical features such as multiple cysts, location in the posterior maxilla, the patient's age, and a higher recurrence rate [9]. Microscopic features indicative

✉ Hirota Muraoka  
muraoka.hirota@nihon-u.ac.jp

<sup>1</sup> Department of Radiology, Nihon University School of Dentistry at Matsudo, 2-870-1 Sakaecho-Nishi, Matsudo, Chiba 271-8587, Japan

of BCNS-associated OKCs include a greater incidence of epithelial budding, epithelial islands, daughter cysts, and odontogenic rests [10, 11]. Computed tomography (CT) and magnetic resonance imaging (MRI) are valuable imaging modalities for evaluating odontogenic cysts and tumors, including OKCs, and their usefulness has been widely reported in previous studies [12–19]. These imaging techniques can provide detailed information on the size, location, and morphology of lesions, which is crucial for diagnosis and treatment planning. Furthermore, many studies have employed diffusion-weighted imaging (DWI) for the quantification and differential diagnosis of lesions, by measuring the random movement of water molecules within biological tissues [20, 21]. However, to our knowledge, few study has yet reported the characteristic imaging findings of BCNS-associated OKCs using multiple imaging modalities across multiple patients, nor has any study compared the apparent diffusion coefficient (ADC) values of OKC in patients with BCNS with those in patients with sporadic OKCs.

This study aimed to evaluate OKCs associated with BCNS using CT and MRI including DWI and to compare them with sporadic cases.

## Materials and methods

### Patients

This retrospective study was approved by our university's ethics committee, and the requirement for obtaining informed consent was waived (EC22-012). The authors investigated five patients (three boys, one girl, and one man; mean age: 12.4 years, range: 9–20 years) with OKCs in the jaw, all of whom had confirmed BCNS between August 2012 and January 2021. Furthermore, 12 patients (10 men, 2 women; mean age: 43.75 years, range: 22–73 years) with sporadic OKCs, including some previously reported patients who underwent MRI examination at our university hospital outpatient clinic between November 2017 and February 2019, were included in the study [13]. Histopathological diagnoses were obtained after surgery for all lesions [22].

### Image acquisition

Panoramic radiography was performed using the Veraviewepocs system (J. Morita Ltd., Kyoto, Japan), set at 10 mA and 60 kV. CT scans were performed using an Aquilion 64 scanner

(Canon Medical Systems, Otawara, Japan) with the parameters 120 kV and 100 mA. The tube current was adjusted using Real EC (Canon Medical Systems, Otawara, Japan), and the reconstructed slice thickness was 0.5 mm. The field of view (FOV) was set at 240 mm × 240 mm, with the gantry angle parallel to the occlusal plane. Images were reconstructed using bone and soft tissue algorithms without contrast material. The bone window had a level of 500 Hounsfield units (HU) and a width of 2800 HU, while the soft tissue window had a level of 30 HU and a width of 300 HU. MRI was performed using a 1.5 T superconductive MRI scanner (Intera Achieva® 1.5 T Nova, Philips Medical Systems, Best, Netherlands) with a five-channel phased array coil. T1-weighted images had repetition time (TR)/echo time (TE) = 550/15 ms, section thickness = 6.0 mm, matrix size = 192 × 256, and FOV = 230 × 260 mm. The parameters for T2-weighted images were TR/TE = 3500/120 ms, section thickness = 6.0 mm, matrix size = 192 × 256, and FOV = 230 × 260 mm. Short-tau inversion recovery (STIR) images were acquired using TR/TE/inversion time (TI) = 2500/60/180 ms, section thickness = 6.0 mm, matrix size = 320 × 256, and FOV = 230 × 195.5 mm. DWI was performed using a single-shot echo-planar sequence with TR/TE = 5100/70, SENSE factor = 2.0, 1566 Hz/pixel bandwidth, section thickness = 6.0 mm, acquisition matrix = 128 × 128, reconstruction matrix = 256 × 256, FOV = 250 × 250 mm, intersection gap = 1.4 mm, 3 acquisitions, imaging time = 3 min 29 s, and b-values = 0 and 1000 s/mm<sup>2</sup>. Apparent diffusion coefficient values were calculated using the formula  $ADC\ value = -\ln(SI(b1)/SI(b2))/(b1-b2)$ , and an ADC map was generated based on the per-voxel ADC values.

### Image analysis

In patients with BCNS, the investigated parameters included the location, size, nature (unilocular or multilocular), border characteristics, jawbone bulging, density (HU on CT), signal intensity, inflammation of surrounding tissue, and ADC values (on MRI) of the lesions. In patients with sporadic OKCs, ADC values were measured. All analyses were performed by a board-certified oral radiologist with 11 years of experience.

### Statistical analysis

First, we checked the normality of the outcome variables using the Shapiro–Wilk test. Patient age and ADC values for BCNS-related OKCs and sporadic OKCs were compared

**Table 1** CT, MRI, and DWI findings of odontogenic keratocysts in patients with basal cell nevus syndrome

Patients number, age, and sex	Site	CT findings					MR findings					DWI findings	
		Size (A-P×R-L×C-C mm)	Unilocular or Multilocular	Border	Jaw-bone bulging	Density	CT value (±SD HU)	SI on T1-weighted image	SI on T2-weighted image	SI on STIR	Inflammation of surrounding tissue	ADC value (±SD ×10 <sup>-3</sup> mm <sup>2</sup> /s)	
1, 12 years (y), girl	Right mandibular molar	24×15.5×23	Unilocular	Clear	+	Low-intermediate	29.84±76.14	Low	Intermediate to high	High	-	1.31±0.06	
	Left maxillary molar	17.5×12.0×12.5	Unilocular	Clear	+	Low-intermediate	46.99±123.28	Low to intermediate	Intermediate to high	Intermediate to high	-	0.92±0.26	
	Right mandibular molar	22.5×11.0×20.5	Unilocular	Clear	+	Low-intermediate	44.71±103.86	Low to intermediate	Intermediate to high	Intermediate to high	-	0.66±0.09	
	Left mandibular incisor	7.5×8.5×7.0	Unilocular	Clear	-	Low-intermediate	142.05±63.06	Low	Intermediate to high	Intermediate to high	-	0.85±0.19	
3, 11 y, boy	Left mandibular molar	11.5×12.0×13.5	Unilocular	Clear	+	Low-intermediate	27.53±90.84	Low	Intermediate to high	High	-	0.83±0.13	
	Right maxillary molar	32.5×27.5×35.0	Unilocular	Clear	+	Low-intermediate	48.94±109.5	Low	Intermediate to high	Intermediate to high	-	0.96±0.18	
	Left maxillary molar	20.5×18.0×21.0	Unilocular	Clear	+	Low-intermediate	50.13±115.74	Low	Intermediate to high	Intermediate to high	-	0.71±0.09	
	Right mandibular molar	48.5×40×59.5	Unilocular	Clear	+	Low-intermediate	27.97±22.43	Low	High	High	+	2.66±0.08	
4, 10 y, boy	Left mandibular molar	26.5×16.5×27.5	Unilocular	Clear	+	Low-intermediate	30.87±159.32	Low	Intermediate to high	High	-	1.25±0.28	
	Right maxillary molar	38.5×36.5×42.5	Unilocular	Clear	+	Low-intermediate	14.88±135.6	Low	High	High	-	1.71±0.18	
	Right mandibular incisor	19×68.0×30.5	Unilocular	Clear	+	Low-intermediate	32.94±79.01	Low to intermediate	Intermediate to high	Intermediate to high	+	0.79±0.12	
	Left Mandibular molar	24.0×17.0×22.0	Unilocular	Clear	+	Low-intermediate	37.41±127.74	Low	Intermediate to high	Intermediate to high	-	1.04±0.16	
Right maxillary incisor	35.5×35.5×34.5	Unilocular	Clear	+	Low-intermediate	55.04±109.69	Low	Low to intermediate	Intermediate to high	Intermediate to high	-	1.35±0.12	

Table 1 (continued)

Patients number, age, and sex	Site	CT findings				MR findings				DWI findings		
		Size (A-P×R-L×C-C mm)	Unilocular or Multilocular	Border	Jaw-bone bulging	Density	CT value (±SD HU)	SI on T1-weighted image	SI on T2-weighted image	SI on STIR	Inflammation of surrounding tissue	ADC value (±SD ×10 <sup>-3</sup> mm <sup>2</sup> /s)
5, 20 y, man	Right mandibular premolar	20.0×11.0×20.0	Unilocular	Clear	-	Low-intermediate	5.76±109.69	Low to intermediate	Low to intermediate	Intermediate	-	0.58±0.1
	Right maxillary molar	12.5×23.0×14.5	Multilocular	Clear	+	Low-intermediate	66.52±121.78	Low to intermediate	Low to intermediate	Intermediate to high	-	0.98±0.12
	Left maxillary molar	26.5×22.5×28.0	Unilocular	Clear	+	Low-intermediate	33.36±109.41	Low to intermediate	Low to intermediate	Intermediate to high	-	0.78±0.12

SD Standard deviation, N/A Not applicable, A-P Anterior–posterior, R-L Right-left, SI Signal intensity

using the t-test or Mann–Whitney U test. Fisher's exact test was used to confirm sex differences between the groups. In these analyses, lesions were treated as predictor variables, while age, sex, and ADC values were treated as outcome variables. Statistical analyses were performed SPSS version 28 (IBM Japan, Tokyo, Japan). Statistical significance was set at  $P < 0.05$ .

### Results

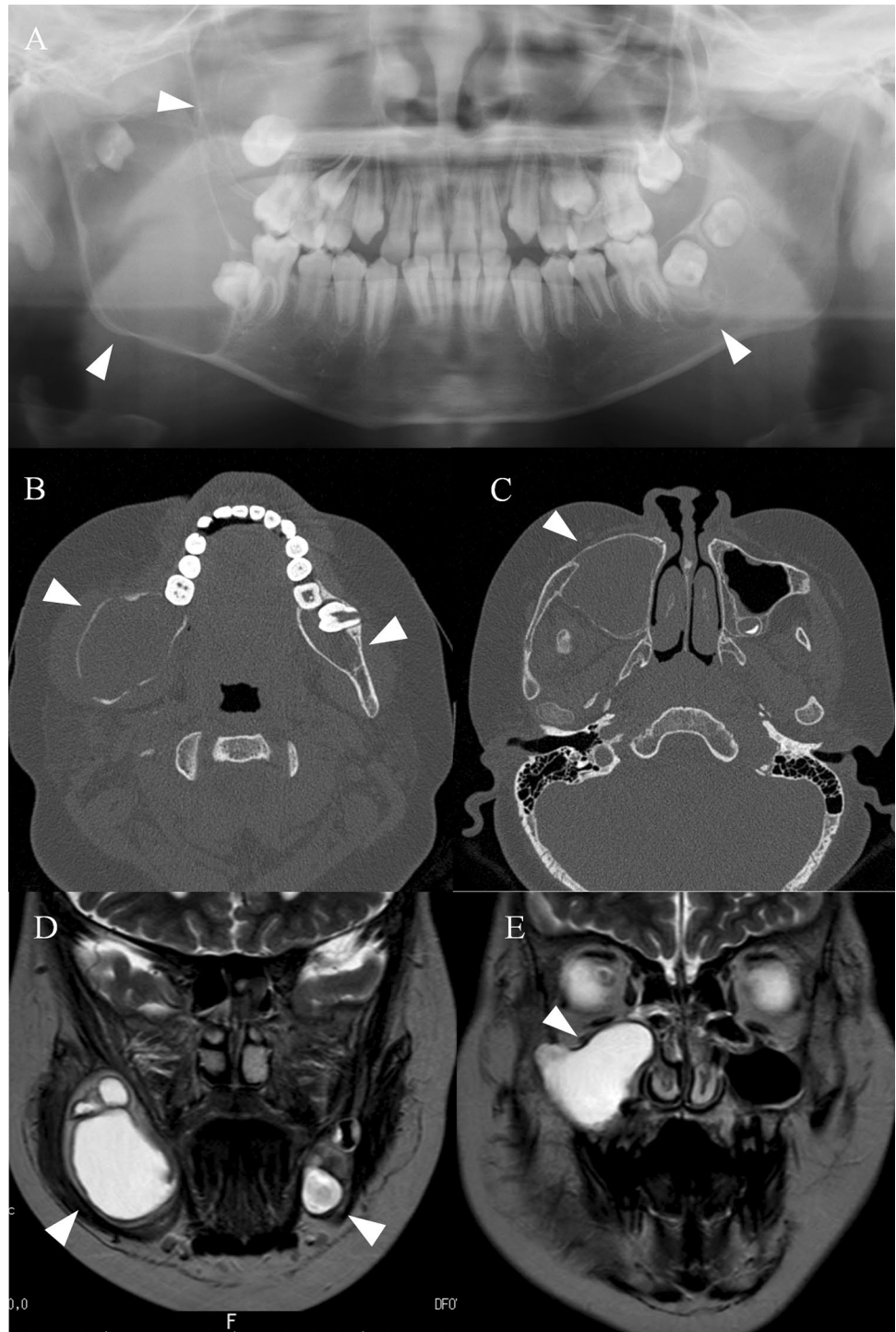
On average, each patient with BCNS had 3.2 lesions. Most lesions (all but one) were unilocular, although the specific site and size of the lesions varied among the patients. All the lesions exhibited clear borders and, except for two, showed jawbone bulging. CT demonstrated low to moderate density in all lesions, with CT values ranging from 5.76 to 142.05 HU. On MRI, nearly all lesions appeared as low signal intensity on T1-weighted images and moderate to high signal intensity on T2-weighted images and STIR sequences. Two relatively large lesions exhibited signal abnormalities in the surrounding soft tissues. DWI provided ADC values ranging from 0.58 to  $2.66 \times 10^{-3}$  mm<sup>2</sup>/s. Table 1 and Figs. 1, 2 and 3 present the imaging findings and images of patients with BCNS investigated in this study. There was no significant correlation between ADC values and age ( $P = 1.0$ ,  $r = 0.158$ ) or CT values ( $P = 1.0$ ,  $r = -0.079$ ). No significant associations were found between ADC values and sex, site, lesion type (unilocular or multilocular), or bone bulging ( $P = 0.6$ , 0.758, 0.875, 0.2, respectively).

Table 2 shows the diagnostic data, demographic data, and ADC value including patients with sporadic OKCs. The ADC values for sporadic OKCs ranged from 0.67 to  $1.11 \times 10^{-3}$  mm<sup>2</sup>/s. The median ADC values [interquartile range (IQR)] were 0.94 [0.79–1.27] and 0.89 [0.81–0.94], corresponding to BCNS-associated OKCs and sporadic OKCs, respectively ( $P = 0.478$ ) (Fig. 4). Additionally, although there was no sex difference between the two groups ( $P = 1.0$ ), the mean age was significantly lower in patients with BCNS ( $P < 0.001$ ).

### Discussion

This study has identified several characteristic findings of OKCs in patients with BCNS. Notably, this study is the first to report the ADC values of OKCs in patients with BCNS, revealing a broader range of ADC values compared to those associated with sporadic OKCs.

**Fig. 1** An 11-year-old boy with BCNS. **a** Panoramic X-ray image reveals two lesions in the mandible and one in the maxilla (arrows). **b, c** Axial CT in bone windows reveals a significant bulging in the jawbone (arrows). **d, e** Coronal magnetic resonance images demonstrate high signal intensity on T2-weighted images (arrows). Abbreviations: BCNS: Basal Cell Nevus Syndrome; CT: Computed Tomography; MR: Magnetic Resonance; T2: T2-weighted imaging



BCNS is also known by various names, including Gorlin–Goltz syndrome, Gorlin syndrome, nevoid basal cell carcinoma syndrome, and syndrome of jaw cysts and jaw

cyst-basal cell nevus-bifid rib syndrome [23, 24]. The syndrome can manifest at various ages, with the onset typically occurring during childhood or adolescence [23, 24]. The

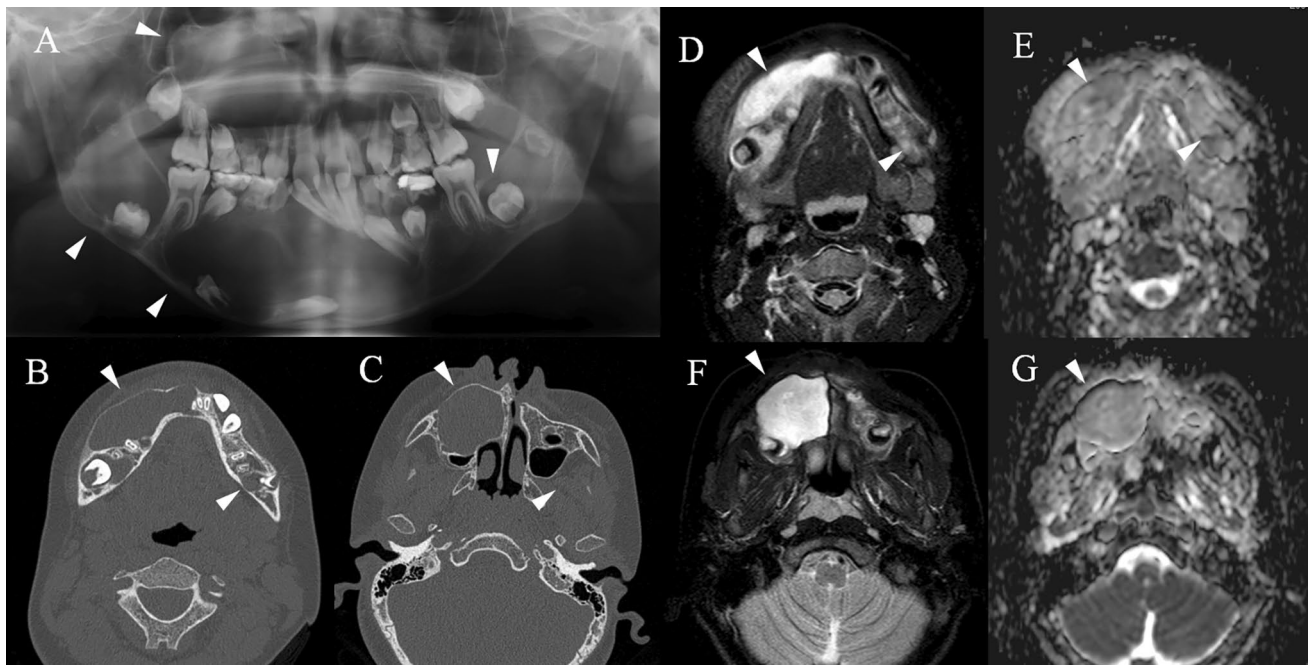


**Fig. 2** A 10-year-old boy diagnosed with BCNS. **a** Panoramic X-ray image reveals two lesions in the mandible and one in the maxilla (arrows). **b, c** Axial CT in bone reveals a significant bulging in the jawbone (arrows). **d, f** Axial and coronal MR images demonstrate intermediate to high signal intensity on STIR images (arrows). **e, g**

ADC maps show diffusion restriction in each lesion (arrows). Abbreviations: ADC: Apparent Diffusion Coefficient; BCNS: Basal Cell Nevus Syndrome; CT: Computed Tomography; MR: Magnetic Resonance; STIR: Short-Tau Inversion Recovery

exact age of onset varies among individuals, but it is commonly observed and diagnosed within the first 20 years of life [1, 2]. BCNS affects both sexes, with no significant predilection for one sex over the other [25]. It is characterized by various clinical features that affect multiple organs and systems [26]. Cutaneous manifestations include the presence of numerous BCCs, which typically appear at an early age and tend to recur [26]. In addition to dermatological findings, BCNS can involve various other structures. Skeletal abnormalities are commonly observed, including bifid ribs, frontal bossing, and calcification of the falx cerebri [27]. Jaw cysts, particularly OKCs, are a hallmark feature of BCNS [9]. These cysts are larger and more aggressive and have a higher recurrence rate than sporadic OKCs [9]. Other oral manifestations may include dental abnormalities, such as missing or supernumerary teeth [26, 28]. Diagnosis of BCNS typically involves a combination of clinical evaluation, genetic testing, and radiological imaging [26]. Early detection and diagnosis of BCNS facilitates timely

intervention and reduces the risk of complications associated with advanced BCC, including local tissue destruction, functional impairment, and disfigurement. However, no study has reported the characteristic findings of BCNS-related OKC using multiple imaging modalities and compared the ADC values of OKC in patients with BCNS with those of sporadic OKC.

Our study included five patients with BCNS who had OKCs in the jaw. The patients' demographic features were consistent with the known tendency of BCNS-associated OKCs to be skewed toward younger age groups but differed by a higher incidence in males [1, 27]. On average, each patient had 3.2 lesions, indicating the multifocal nature of OKCs in patients with BCNS. This observation aligns with previous research, which has demonstrated a tendency for multiple OKCs to develop in individuals with BCNS [29]. Most lesions were unilocular (all but one), a finding consistent with the characteristic radiographic appearance of OKC showing unilocular radiolucency [30]. The specific size of

**Fig. 3** A 9-year-old boy diagnosed with BCNS. **a, b** Axial CT in bone windows reveals a bulging in the jawbone (arrows). **c, e** Axial MR images demonstrate intermediate to high signal intensity on STIR images (arrows). **d, f** ADC maps show diffusion restriction in each lesion (arrows). Abbreviations: ADC: Apparent Diffusion Coefficient; BCNS: Basal Cell Nevus Syndrome; CT: Computed Tomography; MR: Magnetic Resonance; STIR: Short-Tau Inversion Recovery

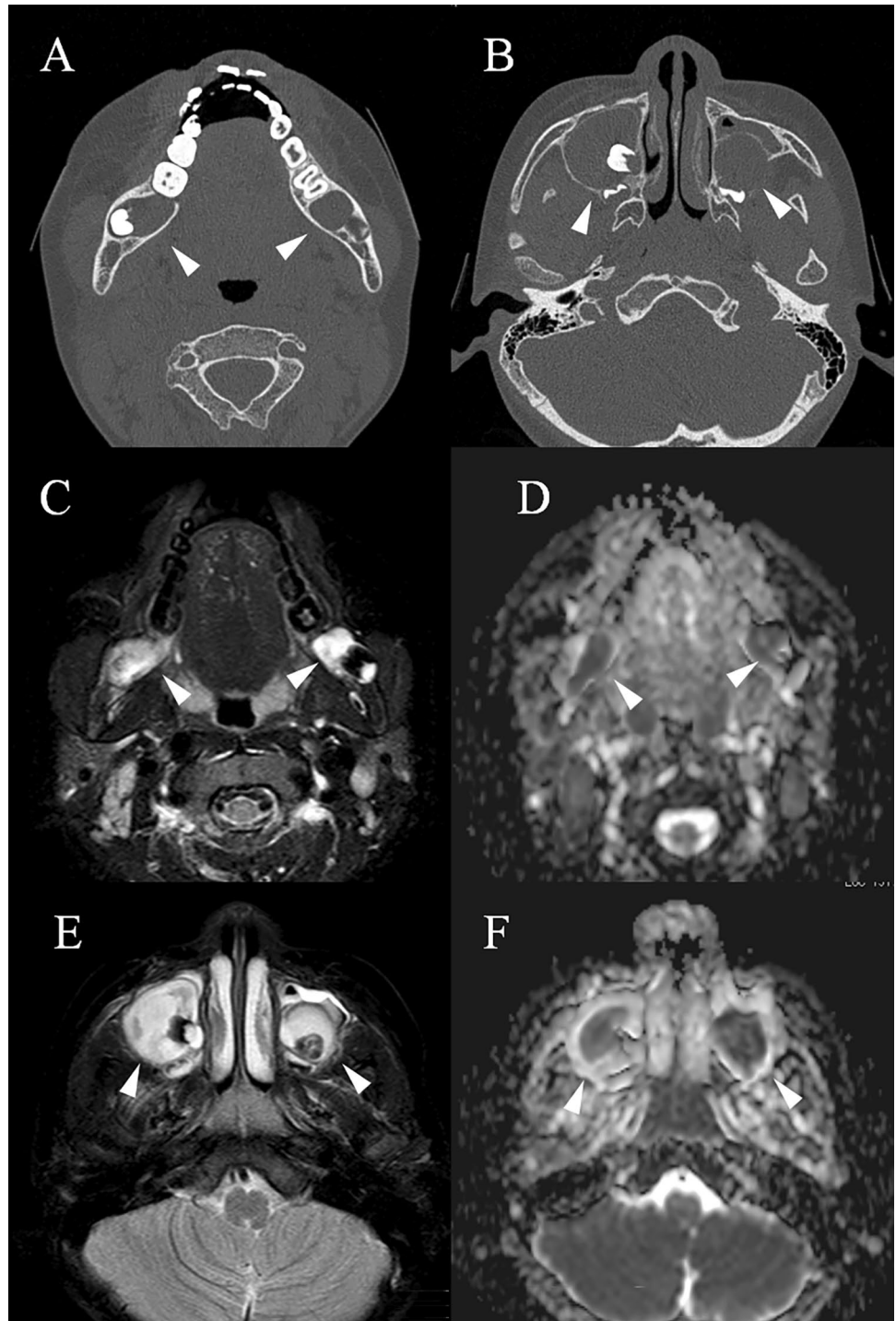


**Table 2** The diagnostic data, demographic data, and ADC value

	BCNS patient with OKCs (n=5)	Patient with sporadic OKCs (n=12)	<i>P</i> -value
Mean Age (years)	12.4	43.75	<.001*
Sex			1.0**
Male (n=14)	4	10	
Female (n=3)	1	2	
Median ADC [IQR]	0.94 [0.79–1.27]	0.89 [0.81–0.94]	.478***

ADC Apparent diffusion coefficient; BCNS: Basal cell nevus syndrome; IQR: Interquartile range

\* t-test, \*\* Fisher's exact test, \*\*\* Mann–Whitney U test

lesions varied among patients. Generally, the OKCs ranged in size from small to large lesions [30]. The ratio of the maxilla to the mandible was 1:1.3. OKCs occurred in different locations within the jaw, including the mandible and maxilla, although previous reports indicated that they were slightly more common in the mandible, consistent with the present report's findings [30]. All the lesions exhibited clear borders, which is a common feature of OKCs. This finding is consistent with that of previous studies that have described well-clear borders as a typical radiographic characteristic of OKCs [30]. Previous studies reported bone swelling in approximately 67% of OKCs, whereas in the present report, bone swelling was observed in all but two (87.5%) lesions. This may be a hallmark of OKC in patients with BCNS [31]. CT imaging demonstrated low to moderate density in all lesions, with CT values ranging from 5.76 to 142.05 HU. On MRI, ADC values ranged from 0.58 to  $2.66 \times 10^{-3} \text{ mm}^2/\text{s}$ . CT and DWI findings were consistent with those of previously reported sporadic OKCs [16, 31]. The density and ADC values likely reflect keratin and fluid within

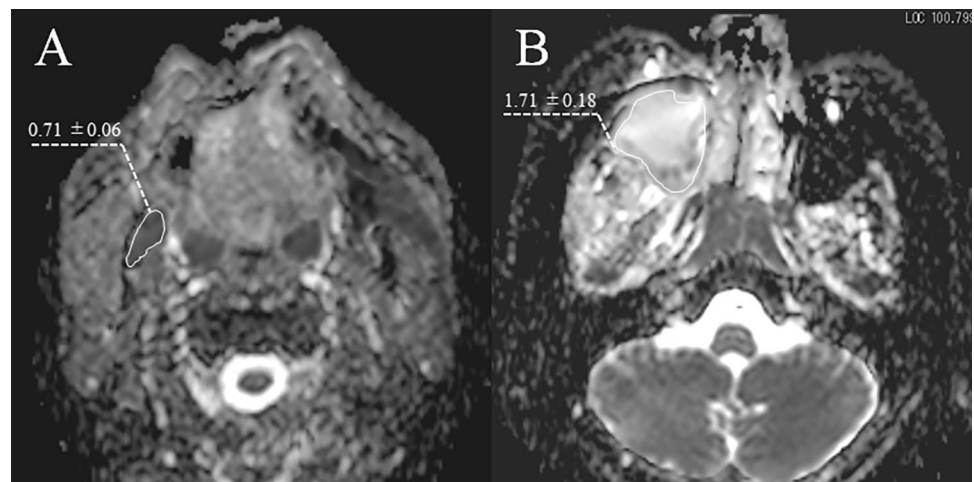
the cyst contents [32,33]. Previous studies reported that the average ADCs for OKC was  $0.954 \times 10^{-3} \text{ mm}^2/\text{s}$ , and the ADC value for a unicystic ameloblastoma and dentigerous cyst was  $\geq 2.150 \times 10^{-3} \text{ mm}^2/\text{s}$  [14, 34]. In the present study, the ADC values in most cases were similar to previously reported ADC values for OKC [13, 32, 33]. However, several cases showed ADC values similar to those of unicystic ameloblastomas and dentigerous cysts, and facilitated diffusion was confirmed. This increase in diffusivity was thought to be due to the low keratin content in a specific lesion [32, 33]. Almost all lesions appeared as low signal intensity on T1-weighted images and moderate to high signal intensity on T2-weighted and STIR images. Two of the larger lesions showed signal abnormalities in the surrounding soft tissue. This finding suggests that the size of the lesion may have affected the surrounding tissue.

ADC values tended to be slightly higher for BCNS-related OKCs than for sporadic OKCs, but there was no clear significant difference between each group. Moreover, the range of values was larger for the ADC values of BCNS-related OKCs than for those of sporadic OKCs. In most sporadic OKCs, ADC values are consistently low owing to keratinisation [14, 32, 34], but in BCNS-related OKCs, there is likely to be significant lesion-to-lesion variation in the amount of keratinisation.

A limitation of our study is the retrospective design, which did not allow for an analysis of the keratin content of each lesion.

In conclusion, this study investigated the characteristic findings of OKCs in patients with BCNS, revealed previously unreported ADC values, and confirmed a wide range of ADC values. These findings provide valuable insights into the radiological features of BCNS-associated OKCs.

**Fig. 4** ADC map indicates the region of interest on the lesion (outline) with the ADC and SD calculated for the region (a: sporadic OKCs, b: BCNS-associated OKC). Abbreviations: ADC: Apparent Diffusion Coefficient; BCNS: Basal Cell Nevus Syndrome; OKC: Odontogenic Keratocyst; SD: Standard Deviation



**Funding** Not applicable.

## Declarations

**Conflict of interest** The authors declare no conflict of interest.

**Ethical approval** We designed and conducted a retrospective cohort study, which was approved by nihon university ethics committee (EC22-012).

**Informed consent** The requirement to obtain written informed consent was waived for this retrospective study. All procedures followed the guidelines of the Declaration of Helsinki, Ethical Principles for Medical Research Involving Human Subjects.

**Animal statements** This article does not contain any studies with animal subjects performed by the any of the authors.

## References

- Gorlin RJ, Goltz RW. Multiple nevoid basal cell epithelioma, jaw cysts and bifid rib syndrome. *New Engl J Med*. 1960;262:908–12. <https://doi.org/10.1056/NEJM196005052621803>.
- Kimonis VE, Goldstein AM, Pastakia B, Yang ML, Kase R, DiGiovanna JJ, et al. Clinical manifestations in 105 persons with nevoid basal cell carcinoma syndrome. *Am J Med Genet*. 1997;69:299–308.
- Johnson RL, Rothman AL, Xie J, Goodrich LV, Bare JW, Bonifas JM, et al. Human homolog of patched, a candidate gene for the basal cell nevus syndrome. *Science*. 1996;272(5268):1668–71. <https://doi.org/10.1126/science.272.5268.1668>.
- Bialer MG, Gailani MR, McLaughlin JA, Petrikovsky B, Bale AE. Prenatal diagnosis of Gorlin syndrome. *Lancet*. 1994;344:477. [https://doi.org/10.1016/s0140-6736\(94\)91810-4](https://doi.org/10.1016/s0140-6736(94)91810-4).
- Bare JW, Lebo RV, Epstein EH. Loss of heterozygosity at chromosome 1q22 in basal cell carcinomas and exclusion of the basal cell nevus syndrome gene from this site. *Cancer Res*. 1992;52:1494–8.
- Witmanowski H, Szychta P, Blochowiak K, Jundzill A, Czajkowski R. Basal cell nevus syndrome (Gorlin-Goltz syndrome): genetic predisposition, clinical picture and treatment. *Postepy Dermatol Alergol*. 2017;34:381–7. <https://doi.org/10.5114/ada.2017.69323>.
- Manfredi M, Vescovi P, Bonanini M, Porter S. Nevoid basal cell carcinoma syndrome: a review of the literature. *Int J Oral Maxillofac Surg*. 2004;33:117–24. <https://doi.org/10.1054/ijom.2003.0435>.
- Karhade DS, Afshar S, Padwa BL. What is the prevalence of undiagnosed nevoid basal cell carcinoma syndrome in children with an odontogenic keratocyst? *J Oral Maxillofac Surg*. 2019;77:1389–91. <https://doi.org/10.1016/j.joms.2019.01.045>.
- Yamamoto T, Ichioka H, Yamamoto K, Kanamura N, Sumitomo S, Shikimori S, et al. Nevoid basal cell carcinoma syndrome: clinical features and implications of development of basal cell carcinoma in skin and keratocystic odontogenic tumor in jaw and their gene expressions. *Asian J Oral Maxillofac Surg*. 2011;23:105–12. <https://doi.org/10.1016/j.ajoms.2011.01.003>.
- Woolgar JA, Rippin JW, Browne RM. A comparative study of the clinical and histological features of recurrent and non-recurrent odontogenic keratocysts. *J Oral Pathol*. 1987;16:124–8. <https://doi.org/10.1111/j.1600-0714.1987.tb01478.x>.
- Antonoglou GN, Sandor GK, Koidou VP, Papageorgiou SN. Non-syndromic and syndromic keratocystic odontogenic tumors: systematic review and meta-analysis of recurrences. *J Craniomaxillofac Surg*. 2014;42:e364–71. <https://doi.org/10.1016/j.jcms.2014.03.020>.
- Abdel Razek AAK. Odontogenic Tumors: Imaging-Based Review of the Fourth Edition of World Health Organization Classification. *J Comput Assist Tomogr*. 2019;43(5):671–678. <https://doi.org/10.1097/RCT.0000000000000896>.
- Muraoka H, Kaneda T, Kondo T, Sawada E, Tokunaga S. Diagnostic efficacy of apparent diffusion coefficient, texture features, and their combination for differential diagnosis of odontogenic cysts and tumors. *Oral Surg Oral Med Oral Pathol Oral Radiol*. 2023;135:928–33. <https://doi.org/10.1016/j.oooo.2023.01.008>.
- Vanagundi R, Kumar J, Manchanda A, Mohanty S, Meher R. Diffusion-weighted magnetic resonance imaging in the characterization of odontogenic cysts and tumors. *Oral Surg Oral Med Oral Pathol Oral Radiol*. 2020;130:447–54. <https://doi.org/10.1016/j.oooo.2020.04.010>.
- Minami M, Kaneda T, Yamamoto H, et al. Ameloblastoma in the maxillomandibular region: MR imaging. *Radiology*. 1992;84:389–93. <https://doi.org/10.1148/radiology.184.2.1620834>.
- Minami M, Kaneda T, Ozawa K, Yamamoto H, Itai Y, Ozawa M, et al. Cystic lesions of the maxillomandibular region: MR imaging distinction of odontogenic keratocysts and ameloblastomas from other cysts. *AJR Am J Roentgenol*. 1996;166:943–9. <https://doi.org/10.2214/ajr.166.4.8610578>.
- Apajalahti S, Kelppe J, Kontio R, Hagström J. Imaging characteristics of ameloblastomas and diagnostic value of computed tomography and magnetic resonance imaging in a series of 26 patients. *Oral Surg Oral Med Oral Pathol Oral Radiol*. 2015;120:118–30. <https://doi.org/10.1016/j.oooo.2015.05.002>.
- Niraj LK, Patthi B, Singla A, Gupta R, Ali I, Dhama K, et al. MRI in Dentistry- A Future Towards Radiation Free Imaging - Systematic Review. *J Clin Diagn Res* 2016;10(10):ZE14–ZE19. <https://doi.org/10.7860/JCDR/2016/19435.8658>.
- Munhoz L, Nishimura DA, Hisatomi M, Yanagi Y, Asaumi J, Arita ES. Application of diffusion-weighted magnetic resonance imaging in the diagnosis of odontogenic lesions: a systematic review. *Oral Surg Oral Med Oral Pathol Oral Radiol*. 2020;130(1):85–100.e1. <https://doi.org/10.1016/j.oooo.2019.11.009>.
- Baba A, Kurokawa R, Rawie E, Kurokawa M, Ota Y, Srinivasan A. Normalized Parameters of Dynamic Contrast-Enhanced Perfusion MRI and DWI-ADC for Differentiation between Posttreatment Changes and Recurrence in Head and Neck Cancer. *AJNR Am J Neuroradiol*. 2022;43:1184–9. <https://doi.org/10.3174/ajnr.A7567>.
- Ota Y, Liao E, Capizzano AA, Kurokawa R, Bapuraj JR, Syed F, et al. Diagnostic Role of Diffusion-Weighted and Dynamic Contrast-Enhanced Perfusion MR Imaging in Paragangliomas and Schwannomas in the Head and Neck. *AJNR Am J Neuroradiol*. 2021;42:1839–46. <https://doi.org/10.3174/ajnr.A7266>.
- Suluk-Tekkesin M, Wright JM. The World Health Organization Classification of Odontogenic Lesions: A Summary of the Changes of the 2022 (5th) Edition. *Turk Patoloji Derg*. 2022;38(2):168–84. <https://doi.org/10.5146/tjpath.2022.01573>.
- Gorlin RJ, Cohen MM, Levin LS. *Syndromes of the Head and Neck*. 3rd ed. New York: Oxford University Press; 1990. p. 372–8.
- Deepa MS, Paul R, Balan A. Gorlin Goltz syndrome: A review. *J Indian Acad Oral Med Radiol*. 2003;15:203–9.
- Bree AF, Shah MR. Consensus statement from the first international colloquium on basal cell nevus syndrome (BCNS). *Am J Med Genet A*. 2011;155A:2091–7. <https://doi.org/10.1002/ajmg.a.34128>.

26. Lo ML. Nevoid basal cell carcinoma syndrome (Gorlin syndrome). *Orphanet J Rare Dis*. 2008;3:32.
27. Kimonis VE, Mehta SG, Digiovanna JJ, Bale AE, Pastakia B. Radiological features in 82 patients with nevoid basal cell carcinoma (NBCC or Gorlin) syndrome. *Genet Med*. 2004;6:495–502. <https://doi.org/10.1097/01.gim.0000145045.17711.1c>.
28. Evans DG, Ladusans EJ, Rimmer S, Burnell LD, Thakker N, Farndon PA. Complications of the naevoid basal cell carcinoma syndrome: results of a population based study. *J Med Genet*. 1993;30:460–4. <https://doi.org/10.1136/jmg.30.6.460>.
29. Lo Muzio L, Nocini PF, Savoia A, Consolo U, Procaccini M, Zelante L, et al. Nevoid basal cell carcinoma syndrome. Clinical findings in 37 Italian affected individuals. *Clin Genet* 1999;55:34–40. <https://doi.org/10.1034/j.1399-0004.1999.550106.x>
30. Kitisubkanchana J, Reduwan NH, Poomsawat S, Pornprasertsuk-Damrongsri S, Wongchuensoontorn C. Odontogenic keratocyst and ameloblastoma: radiographic evaluation. *Oral Radiol*. 2021;37:55–65. <https://doi.org/10.1007/s11282-020-00425-2>.
31. Alves DBM, Tuji FM, Alves FA, Rocha AC, Santos-Silva ARD, Vargas PA, et al. Evaluation of mandibular odontogenic keratocyst and ameloblastoma by panoramic radiograph and computed tomography. *Dentomaxillofac Radiol*. 2018;47:20170288. <https://doi.org/10.1259/dmfr.20170288>.
32. Sumi M, Ichikawa Y, Katayama I, Tashiro S, Nakamura T. Diffusion-weighted MR imaging of ameloblastomas and keratocystic odontogenic tumors: differentiation by apparent diffusion coefficients of cystic lesions. *AJNR Am J Neuroradiol*. 2008;29(10):1897–901. <https://doi.org/10.3174/ajnr.A1266>.
33. Yoshiura K, Higuchi Y, Arijji Y, Shinohara M, Yuasa K, Nakayama E, et al. Increased attenuation in odontogenic keratocysts with computed tomography: a new finding. *Dentomaxillofac Radiol*. 1994;23(3):138–42. <https://doi.org/10.1259/dmfr.23.3.7530666>.
34. Wamasing N, Watanabe H, Sakamoto J, Tomisato H, Kurabayashi. Differentiation of cystic lesions in the jaw by conventional magnetic resonance imaging and diffusion-weighted imaging. *Dentomaxillofac Radiol* 2022;51:20210212. <https://doi.org/10.1259/dmfr.20210212>

**Publisher's Note** Springer Nature remains neutral with regard to jurisdictional claims in published maps and institutional affiliations.

Springer Nature or its licensor (e.g. a society or other partner) holds exclusive rights to this article under a publishing agreement with the author(s) or other rightsholder(s); author self-archiving of the accepted manuscript version of this article is solely governed by the terms of such publishing agreement and applicable law.